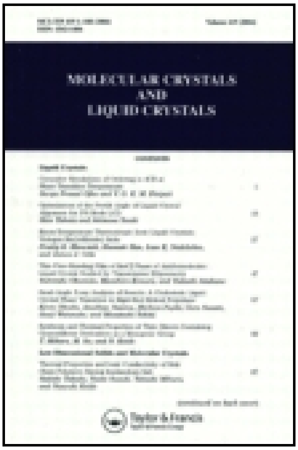

Molecular Crystals and Liquid Crystals
Publication details, including instructions for authors and subscription information:
http://www.tandfonline.com/loi/gmcl16

White and Taylor Type Guest Host Displays Without Scattering Effects Using the Tilted Boundary Conditions

Seigo Togashi [a], Takaharu Suzuki [a], Takaaki Aoyama [a] & Hiroshi Shimizu [a]
[a] Citizen Watch Co. Ltd., Technical Laboratory, Shimotomi, Tokorozawa-shi, Saitama, 359, Japan
Version of record first published: 14 Oct 2011.

To cite this article: Seigo Togashi, Takaharu Suzuki, Takaaki Aoyama & Hiroshi Shimizu (1981): White and Taylor Type Guest Host Displays Without Scattering Effects Using the Tilted Boundary Conditions, Molecular Crystals and Liquid Crystals, 67:1, 117-123

To link to this article: http://dx.doi.org/10.1080/00268948108070881

Mol. Cryst. Liq. Cryst., 1981, Vol. 59, pp. 117–124
0026–8941/81/6704–0117$06.50/0

White and Taylor Type Guest Host Displays Without Scattering Effects Using the Tilted Boundary Conditions

SEIGO TOGASHI, TAKAHARU SUZUKI, TAKAAKI AOYAMA and HIROSHI SHIMIZU

Citizen Watch Co. Ltd., Technical Laboratory, Shimotomi, Tokorozawa-shi, Saitama 359 Japan

(*Received July 29, 1980*)

White and Taylor type guest host displays using the tilted boundary condition have been reported. The parallel or the perpendicular boundary condition is usually used for these displays and both conditions cause scattering phemomena after the electric field removal. The present paper reports the relaxation processes of samples with the tilted boundary after the field removal. Using the tilted boundary, two types of nonscattering conditions depending on the thickness of the liquid crystal layer (d), the natural pitch (Po) and the boundary condition (ϕ) exist. Both types of conditions are discussed in detail.

INTRODUCTION

Compared with the conventional guest host display devices[1] using a non-chiral nematic host, White and Taylor type guest host display devices[2] using a cholesteric host have good contrast and brightness. White and Taylor[2] pointed out that the contrast was higher in a short pitch cholesteric host than in a long pitch one. However, in case of a short pitch system, the transient or the storage scattering states occur during the relaxation from the electric field induced homeotropic state H to the initial planer state G after an electric field is removed. These scattering states reduce the quality of display devices. These relaxation processes strongly depend on the natural pitch of the nematic-cholesteric liquid crystal mixture (Po), the thickness of the liquid crystal layer (d) and the boundary condition at the surface of the liquid crystal

Paper presented at the 8th International Liquid Crystal Conference, Kyoto, Japan, June 30–July 4, 1980.

layer. These phenomena are well investigated in relation to the application to storage type liquid crystal display devices.[3–6] M. Kawachi *et al.*[6] reported that the transient planer state G^* (the helical pitch P is about twice as long as the natural pitch Po) and the transient scattering state G' appear in sequence in the relaxation process from H to G for both samples using the perpendicular boundary condition and the parallel boundary condition.

The present study reports the relaxation process of samples using the tilted boundary condition. The nonscattering condition depending on the liquid crystal layer thickness (d), the natural pitch (Po) and the angle between the parallel component with respect to the substrate of the director on one of the boundary and that on another boundary (ϕ) are discussed.

EXPERIMENTAL

The nematic-cholesteric liquid crystals used were the mixtures of ZLI1132, obtained from E. Merk, and cholesteric nonanoate (CN). The natural pitch of these mixtures were adjusted by varying the concentration of CN, to obtain measured pitch values (Po) in the range approximately 2.5 μm to 20 μm, using the Cano wedge technique.[7] The cells were Cano wedge cells: the liquid crystal layer thickness varied from 4 μm to 32 μm or from 2 μm to 16 μm and uniform gap cells: the liquid crystal layer thickness were 7 ± 0.3 μm or 10 ± 0.3 μm. These values were measured with the white light interference method. The tilted boundary conditions were achieved by depositing SiO film onto the substrates. Controlling the depositing condition, the tilt bias angles of liquid crystal molecules (θo) were approximately 15° and 30°. The tilt bias angles were measured with the magneto capacitance null method.[8] The angle (ϕ) were 0, $\pi/2$, π, $3\pi/2$ for Cano wedge cells and

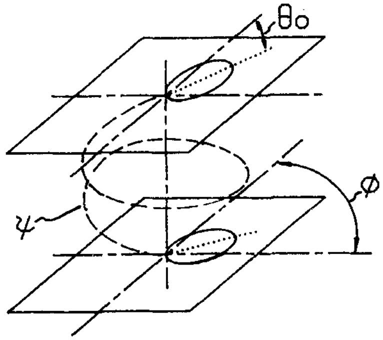

FIGURE 1 Angular relations between the tilt bias angle θo, the rotation angle of molecules ψ, and the angle between both boundaries ϕ.

uniform gap cells, by choosing the depositing direction. The angle (ϕ) and the tilt bias (θo) are explained in Figure 1.

RESULTS AND DISCUSSION

Figure 2 shows one of the example of the texture transition after the field removal, obtained from the time resolved photography of Cano wedge cells. Several milliseconds to several tens milliseconds after the field removal, the first transient planer state G^* appears. In the state G^*, the pitch is aPo ($a = 1.5$–2), the rotation angle (ψ) of liquid crystal molecules between both boundaries takes the same values between $d/Po = (\psi - b_1^*)a/2\pi$ and $(\psi + b_2^*)a/2\pi$: where $b_1^* \fallingdotseq b_2^* \fallingdotseq \pi$ and $\psi = \phi + 2n\pi$ ($n = 0, 1, 2, \ldots$) are only allowed. Several tens milliseconds to several hundreds milliseconds after the field removal, the second transient planer state G^{**} appears. In the state G^{**}, the pitch is equal to the natural pitch Po, ψ takes the same values between $d/Po = (\psi - b_1^{**})/2\pi$ and $(\psi + b_2^{**})/2\pi$: where $b_1^{**} \fallingdotseq b_2^{**} \fallingdotseq \pi$, and $\psi = \phi + 2n\pi$ ($n = 0, 1, 2, \ldots$) are only allowed. Several seconds to several minutes after the field removal, the initial planer state G appears. In the state G, the pitch is Po, ψ takes the same values between $d/Po = (\psi - b_1)/2\pi$ and $(\psi + b_2)/2\pi$: where $b_1 \fallingdotseq b_2 \fallingdotseq \pi/2$, and $\psi = \phi + n\pi$ ($n = 0, 1, 2, \ldots$) are only allowed.

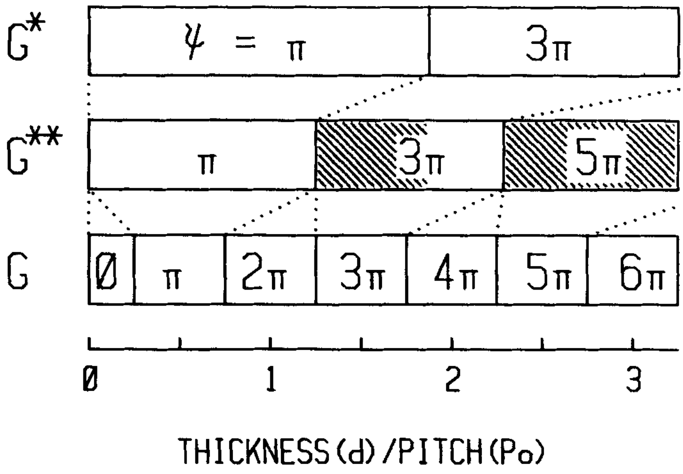

FIGURE 2 The texture transition process after the electric field removal, obtained from time resolved photographs for the Cano wedge cell of $\phi = \pi$, $\theta o = 15°$, $d = 2 - 32$ μm and $Po = 10$ μm. G^* is the first transient state, G^{**} is the second transient state and G is the initial state. Scattering effects exist in the hatching region.

In the state G^*, G^{**}, the rotation $\psi = \phi + (2n + 1)\pi$ ($n = 0, 1, 2, \ldots$) are not allowed. This limitation can be accounted for the anisotropy induced by the tilted boundary condition. As for the parallel component with respect to the substrates of the director orientation on boundaries, both rotation $\psi = \phi + 2n\pi$ and $\phi + (2n + 1)\pi$ match with boundary condition. However, as for the perpendicular component, the rotation $\psi = \phi + 2n\pi$ match with the tilted boundary condition, but the rotation $\psi = \phi + (2n + 1)\pi$ do not match with it. Therefore, the tilt matching rotation ($\psi = \phi + 2n\pi$) are stable and are able to appear in the transient states such as G^*, G^{**}. While, the tilt mismatching rotation ($\psi = \phi + (2n + 1)\pi$) are unstable and only are allowed in the static state such as G. The scattering phenomena depend on the G^* to G^{**} transition. This transition is fast, and when the rotation $\psi(G^*)$ is not equal to the rotation $\psi(G^{**})$, the scattering states appears. While, when $\psi(G^*)$ is equal to $\psi(G^{**})$, the scattering states do not occur. The G^{**} to G transition causes the motion of disclination walls but no scattering phenomena. This transition is slow, and when $\psi(G^{**})$ is not equal to $\psi(G)$, only the motion of disclination walls appear.

Figure 3 shows the texture transition pattern map after the field removal depending on ϕ and d/Po, obtained from the experiment for Cano wedge cells and uniform gap cells. There are three types A, B, C, each has a different

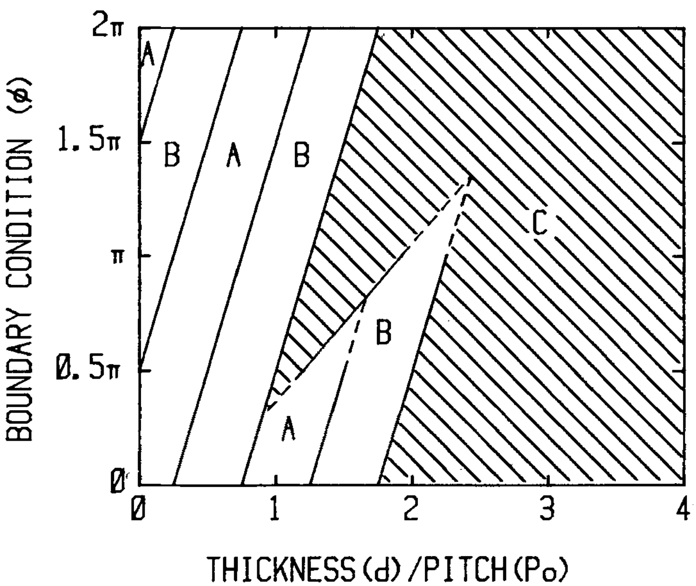

FIGURE 3 The texture transition pattern map depending on ϕ and d/Po after the electric field removal. The transition patterns are classified into 3 types, i.e. A, B, C. Each A, B type has no scattering effects. Scattering phenomena only appear in C type.

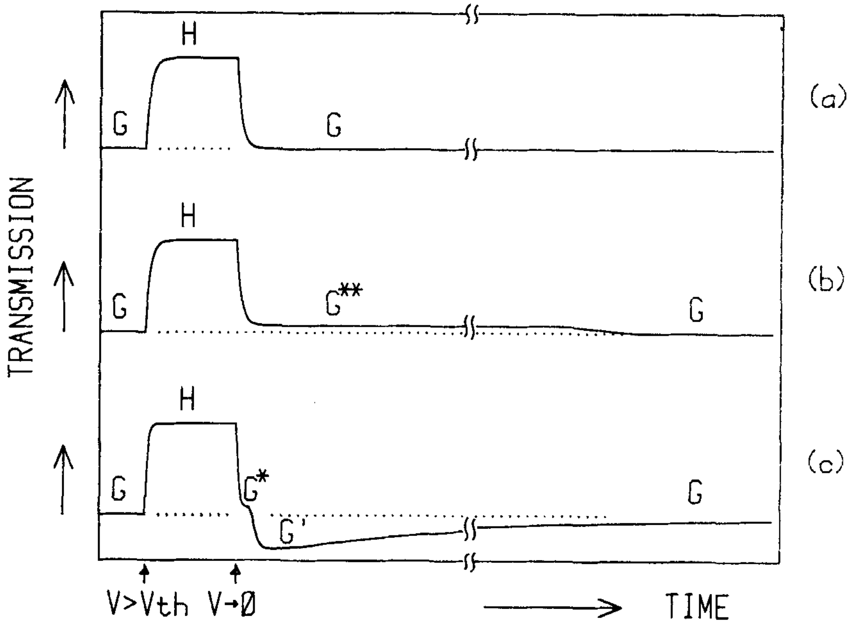

FIGURE 4 The transient characteristics. (a) A type, (b) B type, (c) C type.

relaxation process. Figure 4(a) shows the transient characteristics of A type. This relaxation process has no intermediate state and a direct transition H to G is possible, without any scattering and disclination. In A type region, the boundary condition ϕ and d/Po are matching, and $\psi(G^*) = \psi(G^{**}) = \psi(G)$. Figure 4(b) shows the transient characteristics of B type. In B type region, the boundary condition ϕ and d/Po are mismatching and $\psi(G^*) = \psi(G^{**}) \neq \psi(G)$. On the relaxation process, the state G^{**} with the pitch $p = 2dPo/(2d \pm Po)$ appears at first, and then the state G^{**} relaxes to the state G by the motion of the disclination wall but no scattering phenomena. Figure 4(c) shows the transient characteristics of C type. In C type region, $\psi(G^*) \neq \psi(G^{**}) =$ or $\neq \psi(G)$. This relaxation process is $H \rightarrow G^* \rightarrow G'$ (scattering state) $\rightarrow G$ and it is as same as the process of the samples with the perpendicular or the parallel boundary condition reported by M. Kogure *et al.*[6]

APPLICATION FOR DISPLAY

C type is not suitable for displays unless the scattering phenomena are reduced. However, A, B type are available for displays. Especially, A type is good because of no intermediate transient state during the relaxation.

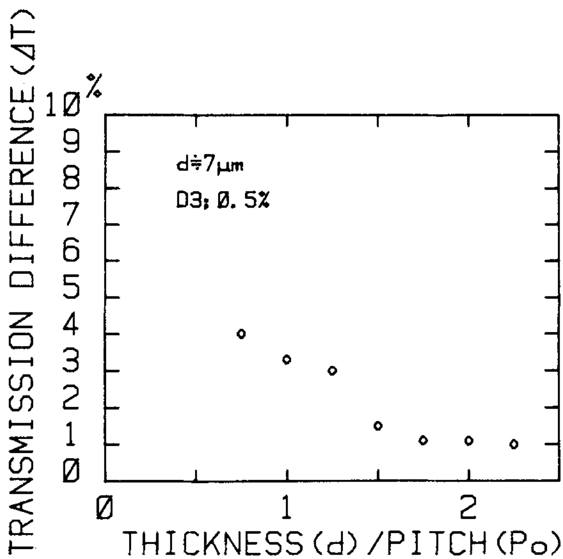

FIGURE 5 ΔT (Transmission differences between G^{**} and G vs d/Po (thickness/natural pitch) characteristics.

However, in A type, the d/Po is limited to a relative low value, i.e. $a(b_1^* + b_2)/2\pi(a - 1)$. If $b_1^* \doteqdot \pi$, $b_2 \doteqdot \pi/2$ and $a \doteqdot 2$–1.5, the maximum d/Po is approximately 1.5–2.2, and the experimental value in Figure 3 is about 1.5. The maximum d/Po in B type is rather high, i.e. $a(b_1^* + b_2^{**})/2\pi(a - 1) \doteqdot 2$–3, where $b_1^* \doteqdot b_2^{**} \doteqdot \pi$, $a \doteqdot 2$–1.5. The experimental value in Figure 3 is about 2.3. From the view-point of contrast, B type is better than A type, because of the higher limitation of d/Po. However, B type has some disadvantages, i.e., the slight uneven contrast and the relatively high driving voltage. The former is caused by the transmission difference ΔT between the state G^{**} and G. Figure 5 shows ΔT vs d/Po characteristics, $d/Po \lesssim 1.5$ the contrast difference is visible, while $d/Po \gtrsim 1.5$ is available for display. The latter disadvantage is caused by the mismatching tilted boundary condition. Figure 6 shows the threshold voltage of both matching and mismatching boundary conditions.

CONCLUSION

Compared with the parallel or the perpendicular boundary condition used for White and Taylor type guest host display, the tilted boundary condition is able to eliminate the scattering phenomena for $d/Po \lesssim 2 - 3$. The non-

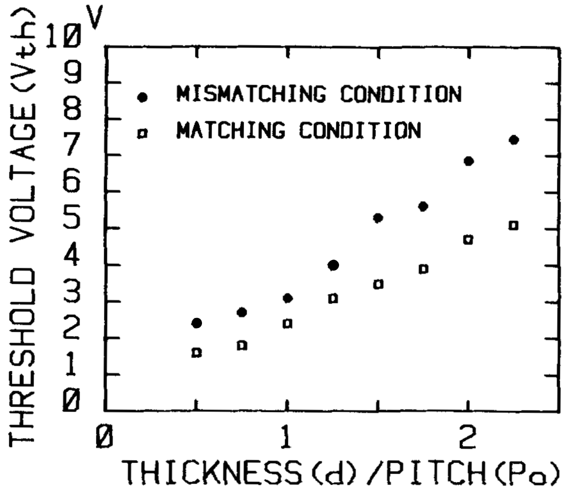

FIGURE 6 *d/Po* dependance of the threshold voltage Vth for two types of boundary conditions.

scattering conditions are classified into two types with *d/Po* and ϕ. One of them has a matching boundary condition and the other has a mismatching boundary condition. The former type can be driven with a low driving voltage and has a simple relaxation process without any intermediate states. The latter one needs a relatively high voltage and has an intermediate state, however it has relatively high contrast.

References

1. G. H. Heilmeier and L. A. Zanoni, *Appl. Phys. Lett.*, **13**, 91 (1968).
2. D. L. White and G. N. Taylor, *J. Appl. Phys.*, **45**, 4718 (1974).
3. T. Ohtsuka and M. Tsukamoto, *Japan. J. Appl. Phys.*, **12**, 22 (1973).
4. R. A. Kashnow, J. E. Bigelow, H. S. Cole, and C. R. Stein, *Appl. Phys. Lett.*, **23**, 290 (1973).
5. M. Kawashi, O. Kogure, S. Yoshii, and Y. Kato, *Japan. J. Appl. Phys.*, **14**, 1063 (1975).
6. M. Kawachi and O. Kogure, *Japan. J. Appl. Phys.*, **16**, 1673 (1977).
7. P. Kassubck and G. Meier, *Liquid Crystal 2* edited by G. H. Brown (Gordon and Breach, New York) pp. 753–762.
8. K. Toriyama and T. Ishibashi, *Nonemissive Electrooptic Displays* edited by A. R. Kmetz and F. K. von Willisen (Plenum, New York, 1976) pp. 145–148.